Control over Multifunctionality in Optoelectronic Device Based on Organic Phototransistor

4 AUTHORS, INCLUDING:

Biswanath Mukherjee
Narasinha Dutt College

25 PUBLICATIONS **384** CITATIONS

SEE PROFILE

Moumita Mukherjee
Indian Association for the Cultivation of Sci…

13 PUBLICATIONS **203** CITATIONS

SEE PROFILE

Control over Multifunctionality in Optoelectronic Device Based on Organic Phototransistor

Biswanath Mukherjee, Moumita Mukherjee, Youngill Choi, and Seungmoon Pyo*

Department of Chemistry, Konkuk University, Seoul, Republic of Korea 143701

ABSTRACT Highly stable, reproducible, photosensitive organic field-effect transistors based on an n-type organic material, copper hexadecafluorophthalocyanine, and two different polymeric gate dielectrics has been reported and their performances have been compared by evaluating the surface/interface properties. The devices produced a maximum photocurrent gain (I_{light}/I_{dark}) of 79 at V_G = 7 V and showed the potentiality as multifunctional optoelectronic switching applications depending upon the external pulses. The switching time of the transistor upon irradiation of light pulse, i.e., the photoswitching time of the device, was measured to be ∼10 ms. On the basis of optical or combination of optical and electrical pulses, the electronic/optoelectronic properties of the device can be tuned efficiently. The multifunctions achieved by the single device can ensure very promising material for high density RAM and other optoelectronic applications. Furthermore, as the device geometry in the present work is not limited to rigid substrate only, it will lead to the development of flexible organic optoelectronic switch compatible with plastic substrates.

KEYWORDS: organic field-effect transistors • polymeric gate dielectric • multilevel data • photoresponse

INTRODUCTION

Optoelectronic devices based on organic semiconductors have been greatly developed in past decade and are of current research interest (1−4). Compared to their inorganic counterpart, these organic semiconductors offer many fundamental advantages which include low cost, lightweight, large area coverage, relatively easy molecular property engineering and mechanical flexibility compatible with plastic substrates. A variety of optoelectronic devices have been fabricated in the past few years, which showed great promise for future applications in information storage and media.

Organic materials have been successfully utilized for the fabrication of high mobility organic field-effect transistors (OFET) (5), high efficiency (exceeding 4%) organic solar cells (6−8), organic/polymer light-emitting diodes (9, 10), and light-emitting OFET with ambipolar transport properties (11, 12). Organic phototransistors (OPT), a new addition to the family of OFETs, has been the recent research interest (13−20). It is a three-terminal optoelectronic device where light can play the role as one of the external electrodes, just as gate electrode in a typical OFET for the generation of photocarriers, in addition to those induced by the gate bias. The other advantages of OPT device include good response time with high current gain (14−17), cheap fabrication method, low processing temperatures, and 3D stacking. Additionally, using the OPT device a high-speed photocontrolled memory device can be realized from efficient transport of charge carriers, which can be achieved through the effective control of the gate bias amplitude and the external light intensity (15, 18, 19).

Because OPT have higher sensitivity and lower noise level than photodiodes, the phototransistors can be efficiently used for light detection and signal magnification in a single device, which is an important optoelectronic integration.

It is quite reasonable to assume that for maximum absorption of incident light and for photoexcitation of the OPT, the rigid and planar device structure should be ideal, which also resulted in large internal conversion quantum yields and high photocurrent densities (21, 22). In the present study, the well-known n-type semiconductor, copper hexadecafluorophthalocyanine ($F_{16}CuPc$), has been used as the active semiconductor for OPT because of its air-stability and good electron-transport properties (23−27). Two different types of polymers, cross-linked poly(4-vinylphenol) (CL-PVP) and poly(4-phenoxy methylstyrene) (P4PMS), have been employed as gate dielectric in order to investigate the effect of surface properties on the performance of OPTs. The mostly used inorganic dielectric, SiO_2, is believed to be very detrimental to n-type devices, because the presence of −OH groups can prevent the accumulation of electrons near the interface. Also, SiO_2 is not suitable for realizing transparent and flexible devices. In this communication, we have fabricated and analyzed the $F_{16}CuPc$ OPTs with CL-PVP or P4PMS as gate dielectric, and their performances have been compared with each other.

In our earlier communication (26), the $F_{16}CuPc$ OPT based on P4PMS gate dielectric has been simply reported by investigating its photoresponse behavior including switching speed and photosensitivity without discussing the effect of surface property of P4PMS. Here, we aim to compare the
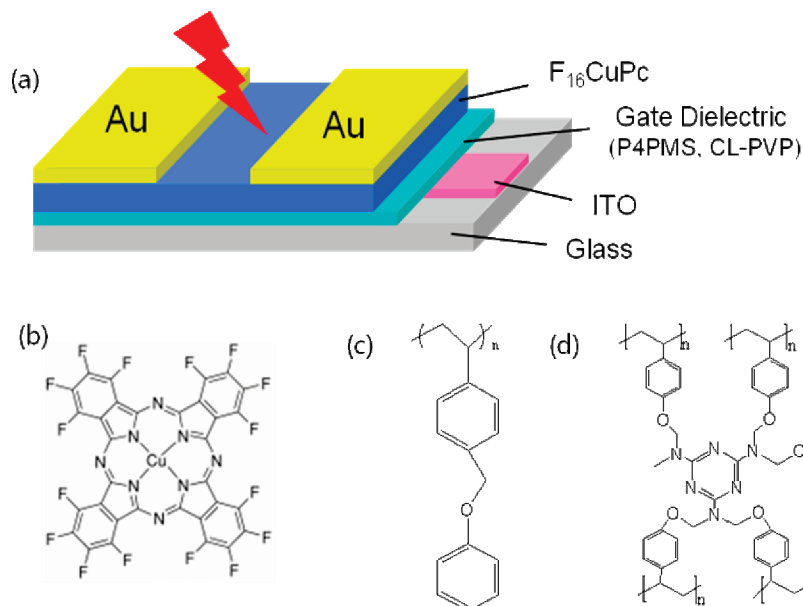
FIGURE 1. (a) Schematic structure of OPT device and the chemical structures of (b) $F_{16}CuPc$, (c) P4PMS, and (d) CL-PVP gate dielectric.

characteristics of $F_{16}CuPc$ OPT based on CL-PVP or P4PMS by examining the interface/surface properties of different gate dielectrics. Though the performance of OPTs (in terms of photoswitching speed and photoresponsivity) looked identical with both types of dielectrics, P4PMS is a better choice as the gate dielectric material as far as mobility, stability, and persistent current is concerned. In addition, we have shown that by suitably integrating the gate bias magnitude and/or incident optical power, it is possible to achieve various types of optical/optoelectronic switches. The optical/optoelectronic control over the electronic performances of the device by suitable choice of input parameters and the multifunctional optoelectronic application, in particular, the multibit optical data recording can be reproduced without any further device complexity and ensured the potential for high density optical random access memory (RAM) and other applications.

EXPERIMENTAL SECTION

The schematic structure of OPT device in this study is shown in Figure 1a. The OPTs were fabricated on cleaned indium tin oxide (ITO)-coated glass substrates which acted as a gate electrode. The active organic semiconductor ($F_{16}CuPc$) as shown in Figure 1b, was purchased from Aldrich Chemical and were used as received. Two different polymer gate dielectrics have been used in this study, namely, cross-linked poly(4-vinyl phenol) (CL-PVP) and poly(4-phenoxy methyl styrene) (P4PMS) as shown in panels c and d in Figure 1, respectively. The CL-PVP precursor solution was prepared by mixing poly(4-vinylphenol) (PVP) (M_w = 20 000 g/mol) (10 wt %) with a cross-linking agent, poly(melamine-co-formaldehyde) (M_n = 511 g/mol) (5 wt %) and butanol (85 wt %) with overnight stirring. P4PMS has been synthesized in-house by the reaction of poly(4-vinylbenzylchloride) and phenol with an aid of K_2CO_3 catalyst in acetone with stirring for 48 h at 80 °C. The reaction mixture was precipitated in the solution of methanol and water and dried for 2 days prior to use. Toluene solution of P4PMS (10 wt %) was spun-cast on the cleaned ITO substrates to get the insulating layer over gate electrode. The spun-cast films were soft baked at 60 °C for 10 min in hot plate and further (hard)

baked at 200 °C/125 °C (CL-PVP/P4PMS) in vacuum oven for 1 h. On top of the dielectrics, organic semiconductor ($F_{16}CuPc$) was deposited (50 nm) through a thermal vacuum deposition method at a rate of 0.2 Å/s and at a base pressure of 5×10^{-6} Torr. Finally, gold (Au) was thermally evaporated on top of the active layer to make the top contact source-drain electrode (40 nm) under a high vacuum (5×10^{-6} Torr) at a rate of 0.3 Å/s. A shadow mask, used during the Au deposition, defined the channel length (L) and channel width (W) as 50 and 1000 μm, respectively. Electrical characterization of the devices were performed at room temperature and under ambient condition using a HP semiconductor parameter analyzer (HP 4145B). For the characterizations of the devices under illumination, a common incandescent lamp (white light) was employed as a light source and the light was illuminated from the top side of the device. The thickness of the gate dielectrics were measured using a surface profiler (AMBIOS XP-100). UV−visible absorption spectrum of $F_{16}CuPc$ in solution was recorded with a CARY 100 (Varian) UV−visible spectrometer.

RESULTS AND DISCUSSION

The output ($I_{DS} - V_{DS}$) characteristics of the OPT based on CL-PVP gate dielectric in dark and under illumination are depicted in Figure 2a. Only characteristics for V_G = 0, 20, and 40 V are shown for clarity. The figure shows typical n-type characteristics with dominant electron transport. With the increase in gate bias (V_G), more charge carriers are accumulated in the interface between $F_{16}CuPc$/CL-PVP near the channel region resulting in increase of the drain current (I_{DS}). Remarkably, after illumination of light in the channel region, I_{DS} increased to a value which is much higher compared to the I_{DS} value under the same V_G in dark condition. Also, the characteristics under the illumination condition retain the same nature as in the dark state. A similar change in output characteristics upon illumination of optical excitation have also been observed in OPT based on P4PMS gate dielectric (26).

Figure 2b illustrates the transfer ($I_{DS} - V_G$) characteristics of the OPT with CL-PVP both in dark and under illumination (5.98 mW/cm^2). The figure clearly displays the enhancement
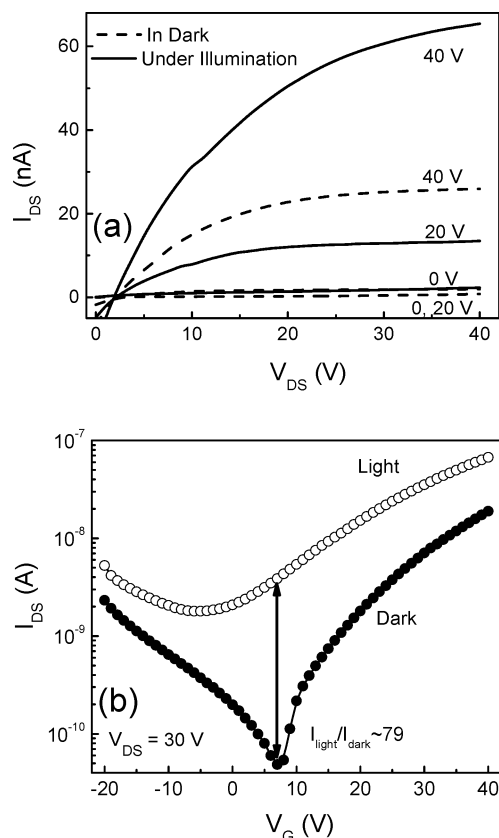
FIGURE 3. Schematic energy level diagram of the OPT under different conditions. (a) No bias ($V_{DS} = 0$ V, $V_G = 0$ V) (b) positive bias ($V_{DS} > 0$ V, $V_G > 0$ V) and (c) positive bias ($V_{DS} > 0$ V, $V_G > 0$ V) with the illumination of light. Energy levels indicated in the figure are not in the scale.

FIGURE 2. Photoresponsive behavior of $F_{16}CuPc$ OPT with CL-PVP having $L = 50$ μm and $W = 1000$ μm. (a) Typical output characteristics of the OFET measured in dark and under white light illumination (5.98 mW/cm^2) are shown. Only three gate voltages ($V_G = 0$, 20, 40 V) are shown for clarity. (b) Transfer characteristics of OFET before and under the illumination. Drain voltage was kept constant at $V_{DS} = 30$ V.

of I_{DS} upon irradiation of light. The ratio between the dark and photo current, I_{light}/I_{dark} at a gate bias of $V_G = 7$ V was measured to be 79. This suggests that the device can be controlled according to the light illumination and the gate bias. The photoresponsivity of the OPT, the typical figure of merit for a phototransistor, at $V_G = 7$ V and at an optical power of 5.98 mW/cm^2 was found to be 1.4 mA/W. In our earlier work, we have observed almost similar photoresponsivity ($\sim$1.5 mA/W) for the OPT based on P4PMS gate dielectric (26). The transfer characteristics of the OPTs in forward and reverse sweep of gate bias, measured both in dark and under illumination, exhibited no hysteresis behavior. The charge carrier mobility (μ) and the threshold voltage (V_{Th}) of the OPT fabricated in this study were estimated to be $\sim$5.32 × 10^{-4} cm^2 V^{-1} s^{-1} and 4.6 V ($F_{16}CuPc$ OPT with P4PMS) and 1.05 × 10^{-4} cm^2 V^{-1} s^{-1} and 9.05 V ($F_{16}CuPc$ OPT with CL-PVP), respectively. This difference in the mobility can be attributed to the morphological differences in the $F_{16}CuPc$ layer caused by different interfacial interactions with the gate dielectrics. It has been found from the tapping mode Atomic Force Microscopic (AFM) image that an average grain size of $F_{16}CuPc$ is larger on P4PMS (31.25 nm) than that on CL-PVP surface (21.48 nm). The more hydrophobic P4PMS surface (discussed in the next section) may help forming active layer of $F_{16}CuPc$ with high structural organi-
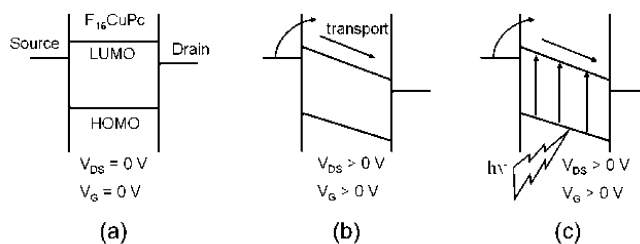
zation and hence larger crystalline size leading to higher carrier mobility (27).

As the characteristics of phototransistor is solely controlled by the number of photogenerated charge carriers, the device efficiency is strongly dependent on the amount and wavelength of the light absorbed by the material. The maximum UV−visible absorption peak of $F_{16}CuPc$ in N-methyl pyrrolidone (NMP) solution is observed in the visible region around 675 nm (26). The bandgap of the material, calculated from the long wavelength edge of the spectrum, was found to be 1.6 eV, which agrees well with the reported value (28). These imply that upon illumination of light, molecules are easily excited and additional mobile charge carriers (photocarriers) are generated viz. holes in the highest occupied molecular orbital (HOMO) and electrons in the lowest unoccupied molecular orbital (LUMO) levels, leading to increase in bulk conduction in the active layer. The photoinduced holes may be immediately trapped in the bulk and interface regions and electron transport is dominated.

The performance of the OPT in dark and under illumination can simply be understood by the energy level diagram depicted in Figure 3. Three different conditions have been illustrated in Figure 3; in a, no bias is applied ($V_{DS} = 0$ V and $V_G = 0$ V), in b, positive bias is applied ($V_{DS} > 0$ V and $V_G > 0$ V), and in c, positive bias ($V_{DS} > 0$ V and $V_G > 0$ V) is applied with the illumination of light. When positive V_{DS} is applied (condition b), electrons from the source electrode will be injected to the lowest unoccupied molecular orbital (LUMO) of $F_{16}CuPc$, leading to the current flow through the device. Furthermore, if light with a photon energy equal to or higher than the band gap energy of $F_{16}CuPc$ is illuminated on the OPT (condition c), in addition to the injected electrons from the electrode, a number of excitons, subsequently electrons and holes, are generated. The electrons from highest occupied molecular orbital (HOMO) of the molecules will be excited to the LUMO of $F_{16}CuPc$ resulting in increase in carrier concentration and hence increase in I_{DS} value. As long as the light is turned on, these additional photogenerated carriers contributed to the conductivity. When the light was turned off, the device regains the dark conductivity. This further indicates that light can play a role as an additional terminal that optically controls device operation along with the conventional three terminals: source, drain, and gate electrodes.

Figure 4 shows the photoswitching performance of the OPT with CL-PVP as the gate dielectric for different gate
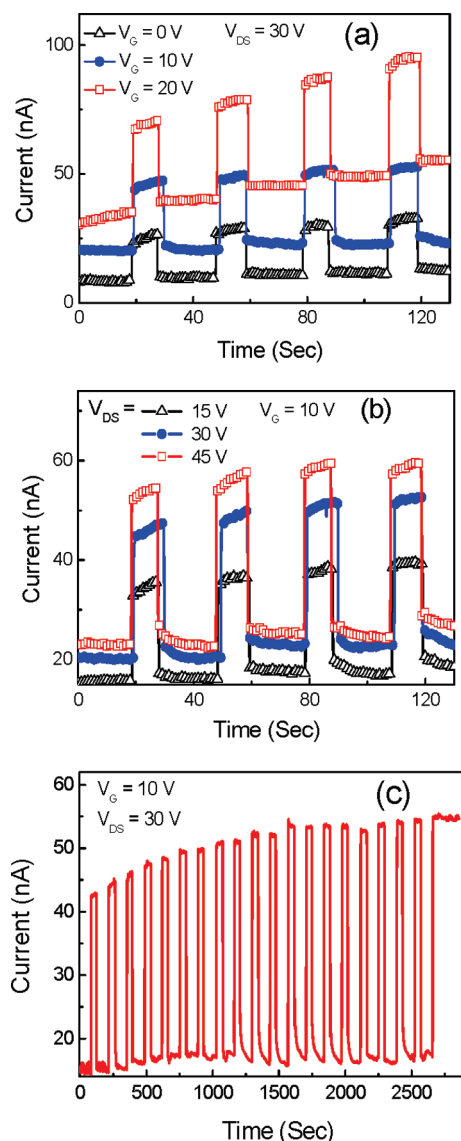
FIGURE 4. Dynamic photoresponse behavior of F$_{16}$CuPc OPT with CL-PVP as gate dielectric illuminated by white light with optical power of 5.66 mW/cm^2. The pulsed light cycles were radiated for 10 s. Photocurrent was measured with time for (a) different V_G with fixed V_{DS} = 30 V and (b) for different V_{DS} with fixed V_G = 10 V. (c) Endurance and stability test of the OPT at fixed V_{DS} = 30 V and V_G = 10 V with optical power of 5.66 mW/cm^2.

voltages. By switching the light on/off, the OPT was capable of switching on/off reversibly with very fast response time demonstrating a two bit storage ("0" or "1") in the OPT. To monitor the photocurrent of the devices in real time, as shown in Figure 4, we measure the drain current as a function of time while it was held at different gate and drain voltages by switching on/off light. Time responses of the OPT have been measured under constant V_{DS} = 30 V and V_G was held constant at 0, 10, 20 V (Figure 4a). In the measurement, light (optical power 5.66 mW/cm^2) was turned on for 10 s and off for 20 s. Each photoresponse cycle consists of three transient regimes—a sharp rise, steady state, and sharp decay.

Here, we have observed a little persistent (remnant) conductivity in the measured photocurrent of the OPT with CL-PVP gate dielectric. However, this behavior is not un-

usual, and common in OPT based on CL-PVP as reported by other groups (29, 30). The increase in I_{DS} with time may be attributed to the absorption of water molecules in the surface of CL-PVP dielectric which enhances the surface polarization, and hence the accumulation of extra charges within the interface between the CL-PVP and F$_{16}$CuPc increases the current with time. This slow and gradual increase in current with time, i.e., the persistent conductivity, however, could be reduced by decreasing the magnitude of V_G. The OPT with P4PMS gate dielectric, on the other hand, exhibit almost no persistent conductivity (26). This may be due to different surface properties of P4PMS from that of CL-PVP. The water contact angles on the surface of P4PMS and CL-PVP were measured to be around 102 and 70°, respectively, indicating that P4PMS is much more hydrophobic than CL-PVP (27). This means that the phenoxy methyl ($-CH_2OC_6H_5$) group introduced at position 4 makes the surface of P4PMS more hydrophobic and prohibits the absorption of water to the dielectric leading to the dramatically reduced persistent conductivity. Furthermore, P4PMS does not have any $-OH$ groups that might act as a charge (electron) trapping site, causing device performance degradation when it is operated under ambient conditions for long time (30). We, therefore, conclude that in view of the persistent current and stability of the OPT, P4PMS could be a better choice for gate dielectric material as compared to CL-PVP. The fast response time in the current OPT makes it suitable for high speed switching and storage device.

To investigate the effect of drain voltage on the photoconductivity of the OPT, we have measured the drain current with time for various values of constant drain bias (V_{DS} = 15, 30, 45 V) keeping gate bias fixed (V_G = 10 V) throughout the whole measurement. The results are shown in Figure 4b. Here the light is switched on for 10 s and off for 20 s. Upon irradiation of light (5.66 mW/cm^2), a large increase in the I_{DS} is observed, which further increased with an increase in the magnitude of V_{DS}. However, once V_{DS} reached the saturation value (beyond 30 V) further increase in V_{DS} values produces only small changes in the photocurrent. This might be due to the constant number of photocarriers generated at a particular optical power input. After a certain V_{DS} when all the photocarriers became transported, the photocurrent becomes saturated. Upon turning off the light source, I_{DS} immediately reached the dark current value, thus eliminating the need of any further gate bias to reduce I_{DS} of any intermediate state (often observed after immediate switching off light) to the initial dark value (15). The devices also exhibited high reproducibility and retention ability. After several tens of cycles, no degradation was observed. Figure 4c shows a representative result for the stability and retention ability of the OPT. It can be seen from the figure that even after more than 45 min of irradiation of light pulses, the device performance is very steady and stable and did not show any sign of degradation. The measured photocurrent, after initial increase, soon settles down to a saturated value.
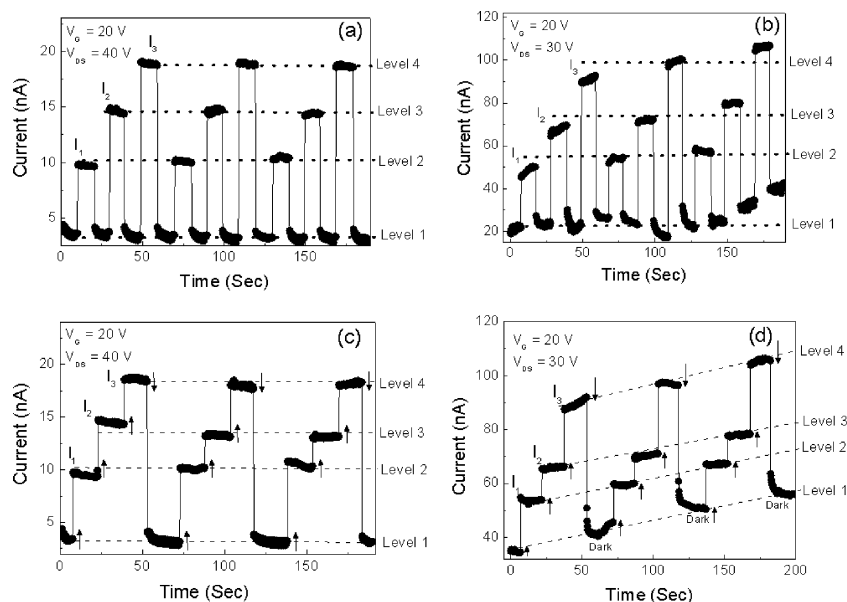
FIGURE 5. Multilevel photoconductance by optical writing with different intensity of light pulses. (a, c) Results for OPT with P4PMS, (b, d) results for OPT with CL-PVP. The fixed bias applied in the two OPTs are $V_{DS} = 40$ V and $V_G = 20$ V for OPT with P4PMS and $V_{DS} = 30$ V and $V_G = 20$ V for OPT with CL-PVP. Light was turned on for 10 s in each of the photoinduced level and then turned off for 10 s before changing to the next intensity level (a and b only). In c and d, the light was kept on (10 s) before changing to next higher intensity level. Here, I_1, I_2, and I_3 correspond respectively to 4.13, 5.5, and 5.98 mW/cm^2. Arrows indicate the time of turning on/off the light pulse.

As the performances of phototransistors are based on photogenerated carriers, the efficiency of the devices is associated to the amount of light absorbed by the active materials. Furthermore, the device efficiency also depends on exciton dissociation into free carriers (electrons and holes), their diffusion and transportation to respective electrodes. Because the density of photogenerated carriers depend on the intensity of the incident light, it is possible to control the photo conductance of the OPT by suitably controlling the incident illumination. To realize the multilevel photo conductance state or multibit data recording in our OPTs, we have adopted optical/optoelectronic "writing" and electronic "reading" process. In addition to the optoelectronic integration of two key parameters, the nonidentical nature of pump- and probe techniques is further advantageous in the sense that it reduces the possibility of perturbation of the probing method to the written bits. In the first method, "writing" of data is achieved by optical pulse only, where we have changed only the illumination intensity (power) of the input light pulse for creating different conductivity (data) level, keeping both V_{DS} and V_G at fixed values. Between two consecutive optical pulses of different intensity, we have either turned the light off or kept it on, demonstrating yet another way to achieve a multilevel photoconductance state. The results have been summed up in Figure 5, where we have presented the results for both OPT with P4PMS (a and c) and CL-PVP (b and d). A clear difference between the photoinduced levels can be observed, where the light pulse was turned on/off for 10 s. When the light was turned off between two consecutive pulses, the devices immediately regain the dark conductivity (Figure 5a) demonstrating fast response speed of the devices. Here also, in the devices based on CL-PVP (Figure 5b), a persistent conductivity was observed. However, in P4PMS-based de-

vice (Figure 5a), the current levels are steady and stable and no persistent conductivity has been noticed. Because the photomemory as demonstrated above always requires the refreshing pulses, that is, the memory is retained as long as the pulse is on, this type of memory can be termed as volatile memory.

In panels c and d in Figure 5, we have shown that a number of different conducting levels (levels 1−4) can also be created in both OPT by sequential increment of the illumination intensity (without turning off the light between two photoinduced levels) with constant V_{DS} and V_G. For OPT with P4PMS, fixed voltages were $V_{DS} = 20$ V, $V_G = 40$ V (Figure 5c), whereas in CL-PVP based device, V_{DS} and V_G were kept constant at 20 and 30 V, respectively (Figure 5d). The cycles can be repeated reproducibly and reversibly without any noticeable degradation in the device performance. Here, with increase in intensity of the "write" (optical) pulse, the density of photogenerated carriers increased and resulted in different levels of conductivity in the devices. Since the illumination intensity for a particular data level is fixed, the number of photogenerated carriers for that level are also constant resulting in almost constant current. The results hence show that different high conductivity levels can be introduced optically by applying "write" pulses of different illumination intensity and the states can be "read" electronically for multifunctional optoelectronic switching applications.

In the second method, we have used a light-assisted pulse voltage program, keeping the intensity of illumination fixed and varied V_G with a fixed V_{DS} value. We have shown that a state could be written with an electrical/optical pulse and read with an electrical pulse by measuring the current of the written state. The results for OPT with P4PMS (Figure 6a) and CL-PVP (Figure 6b) indicate that different conducting
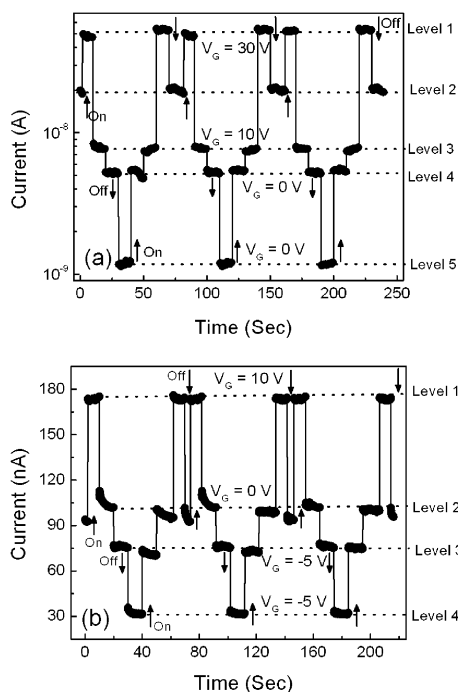
FIGURE 6. Demonstration of multibit data recording by optoelectronic integration. Results for OPTs with dielectric layer of (a) P4PMS and (b) CL-PVP at fixed V_{DS} = 40 V. Different V_G values applied in different steps are indicated in the figure. Turning light on/off is indicated by arrows. Three cycles are shown in both panels.

levels can be induced by suitable integration of the light pulses and the gate bias. V_{DS} value (40 V) and the illumination intensity (5.98 mW/cm^2) was kept fixed throughout the measurement, whereas the V_G value was changed to induce different conducting levels. The figure also indicates that many more conducting levels can be created by optimizing the operating conditions, which will effectively enhance the operational flexibility of the optoelectronic switch. The results, in turn, indicated that the device can efficiently be used as a volatile memory element, which may be useful for most forms of modern random access memory including dynamic random access memory (DRAM) and static random access memory (SRAM).

In an attempt to measure the photoresponse speed of the OPT, we have varied the duration of the optical pulse, with V_{DS} and V_G values both kept fixed at a particular value. In the measurement for OPT with CL-PVP, we have chosen V_{DS} = 40 V and V_G = 20 V, and the voltages were kept fixed throughout the experiment. The optical pulse width, i.e., the time during which the light was turned on, was changed with a mechanical shutter. The results are summarized in Figure 7. It can be seen from the figure that as soon as the light was turned on, the current sharply increased to a high value and remained constant until the optical power is on. The maximum current level is, however, the same for all the measured pulse widths. We have reduced the optical pulse width as small as 0.29 s, but did not find any changes in the current values. To clearly visualize the rise and decay of photocurrent, we have plotted the results for shortest pulse duration (0.29 s) with time scale in the top axis. The results indicate that the photoresponse speed of the current
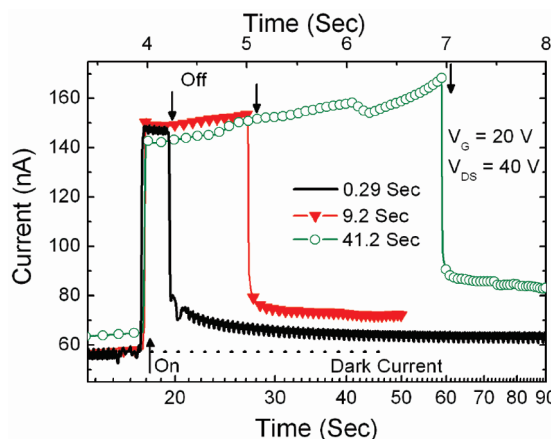

FIGURE 7. Transient behavior of drain current (I_{DS}) of OPT with CL-PVP upon illumination of optical power of different time duration. Optical pulses (5.66 mW/cm^2) were turned on for 0.29, 9.2, and 41.2 s with fixed V_G = 20 V and V_{DS} = 40 V. Time scale for 0.29 s pulse duration has been shown in top axis for clarity.

OPT is well below 1 s. In particular, the photoresponse speed of the OPT is found to be less than 10 ms, which we could not accurately measure due to the instrumental limitations. Nevertheless, this speed is sufficient for the current optoelectronic applications and has enough scope to improve the switching speed of the device. The decay of the photo current upon termination of light is a rather slow process, which we ascribe to the slow nature of recombination of charge carriers, which is limited by the poor recombination cross-section of the trapped holes within the depletion region in presence of the field (15). The decay time of the OPT device is measured to be ~30 ms. Similar values for the photoswitching speed and decay time have been observed for OPT with P4PMS gate dielectric layer (26).

CONCLUSIONS

In conclusion, high photosensitive, multifunctional OPTs were fabricated using two different dielectrics and the performances have been compared. The photoresponsivity and the photoswitching speed of the OPT has been found to be similar with two dielectric materials, but in view of the mobility, persistent current and stability of the OPT, P4PMS has been found to be the better choice for gate dielectric material as compared to CL-PVP. The dependence of the photocurrent on the illumination intensity or on the gate/drain voltages showed that efficient photocarriers could be generated and a large photocurrent gain could be obtained in the current OPTs upon suitable combination of these input parameters. The switching speed of the phototransistor is measured to be well below 10 ms and have a photosensitivity of ~1.5 mA/W. The devices exhibited excellent stability and reproducibility with retention time for more than 45 min. The multifunctions such as photodetection, photoswitching, multilevel data recording, and signal amplification achieved by the single device can ensure very promising material for future optoelectronic applications. Furthermore, the current OPT device, after further investigation and optimization, can potentially be applied for high-density optoelectronic memory devices.

REFERENCES AND NOTES

(1) Facchetti, A.; Yoon, M. H.; Marks, T. *Adv. Mater.* **2005**, *17*, 1705–1725.

(2) Reichmanis, E.; Katz, H.; Kloc, C.; Maliakal, A. *Bell Labs Tech. J.* **2005**, *10*, 87–105.

(3) Sirringhaus, H. *Adv. Mater.* **2005**, *17*, 2411–2425.

(4) Forrest, S. R. *Nature* **2004**, *428*, 911–918.

(5) Dimitrakopoulos, C. D.; Malenfant, P. R. L. *Adv. Mater.* **2002**, *14*, 99–117.

(6) Shaheen, S. E.; Brabec, C. J.; Sariciftci, N. N.; Padinger, F.; Fromherz, T.; Hummelen, J. C. *Appl. Phys. Lett.* **2001**, *78*, 841–843.

(7) Wienk, M. M.; Kroon, J. M.; Varhees, W. J. H.; Knol, J.; Hummelen, J. C.; Van Hal, P. A.; Jansen, R. A. J. *Angew. Chem., Int. Ed.* **2003**, *42*, 3371–3375.

(8) Wienk, M. M.; Kroon, J. M.; Varhees, W. J. H.; Knol, J.; Hummelen, J. C.; Van Hal, P. A.; Jansen, R. A. J. *Angew. Chem.* **2003**, *115*, 3493–3497.

(9) Friend, R. H.; Gymer, R. W.; Holmes, A. B.; Burroughes, J. H.; Marks, R. N.; Taliani, C.; Bradley, D. D. C.; Dos Santos, D. A.; Bredas, J. L.; Logdlund, M.; Salaneck, W. R. *Nature* **1999**, *397*, 121–128.

(10) Coakley, K. M.; McGehee, M. D. *Chem. Mater.* **2004**, *16*, 4533–4542.

(11) Hepp, A.; Heil, H.; Weise, W.; Ahles, M.; Schmechel, R.; Seggern, H. *Phys. Rev. Lett.* **2003**, *91*, 157406.

(12) Cornil, J.; Bredas, J.; Zaumseil, J.; Sirrinhaus, H. *Adv. Mater.* **2007**, *19*, 1791–1799.

(13) Liu, C.-Y.; Bard, A. J. *Acc. Chem. Res.* **1999**, *32*, 235–245.

(14) Jiang, H.; Yang, X.; Cui, Z.; Liu, Y.; Li, H.; Hu, W. *Appl. Phys. Lett.* **2009**, *94*, 123308–123310.

(15) Dutta, S.; Narayan, K. S. *Adv. Mater.* **2004**, *16*, 2151–2155.

(16) Ye, R.; Baba, M.; Mori, K. *Jpn. J. Appl. Phys.* **2005**, *44*, L581–L583.

(17) Saragi, T. P. I.; Pudzich, R.; Fuhrmann, T.; Salbeck, J. *Appl. Phys. Lett.* **2004**, *84*, 2334–2336.

(18) Tang, Q.; Li, L.; Song, Y.; Liu, Y.; Li, H.; Xu, W.; Liu, Y.; Hu, W.; Zhu, D. *Adv. Mater.* **2007**, *19*, 2624–2628.

(19) Cho, M. Y.; Kim, S. J.; Han, Y. D.; Park, D. H.; Kim, K. H.; Choi, D. H.; Joo, J. *Adv. Funct. Mater.* **2008**, *18*, 2905–2912.

(20) Guo, Y.; Du, C.; Yu, G.; Di, C.; Jiang, S.; Xi, H.; Zheng, J.; Yan, S.; Yu, C.; Hu, W.; Liu, Y. *Adv. Funct. Mater.* **2010**, *20*, 1019–1024.

(21) Wohrle, D.; Meissner, K. *Adv. Mater.* **1991**, *3*, 129–138.

(22) Mende, L. S.; Fechtenkotter, A.; Mullen, K.; Moons, E.; Friend, R. H.; MacKenzie, J. D. *Science* **2001**, *293*, 1119–1122.

(23) Oh, Y.; Pyo, S.; Yi, M.; Kwon, S. *Org. Electron.* **2006**, *7*, 77–84.

(24) Bao, Z.; Lovinger, A.; Brown, J. *J. Am. Chem. Soc.* **1998**, *120*, 207–208.

(25) Ye, R.; Baba, M.; Mori, K. *Jpn. J. Appl. Phys.* **2005**, *44*, L581–L583.

(26) Mukherjee, B.; Mukherjee, M.; Choi, Y.; Pyo, S. *J. Phys. Chem. C* **2009**, *113*, 18870–18873.

(27) Mukherjee, M.; Mukherjee, B.; Choi, Y.; Sim, K.; Do, J.; Pyo, S. *Synth. Met.* **2010**, *160*, 504–509.

(28) Shen, C.; Kahn, A. *J. Appl. Phys.* **2001**, *90*, 4549–4554.

(29) Chuang, C. S.; Chen, F. C.; Shieh, H. P. D. *Org. Electron.* **2007**, *8*, 767–772.

(30) Jung, T.; Dodabalapur, A.; Wenz, R.; Mohapatra, S. *Appl. Phys. Lett.* **2005**, *87*, 182109–182111.

AM100127Q